Soft Matter

Accepted Manuscript

ROYAL SOCIETY OF CHEMISTRY

www.rsc.org/softmatter

Soft Matter

RSCPublishing

ARTICLE

Amyloid-like fibrils formed from intrinsically disordered caseins: physicochemical and nanomechanical properties

Cite this: DOI: 10.1039/x0xx00000x

Received ooth April 2015,
Accepted ooth xxxx 2015

DOI: 10.1039/x0xx00000x

www.rsc.org/

Kang Pan and Qixin Zhong*

Department of Food Science and Technology, University of Tennessee in Knoxville, USA.

*E-mail: qzhong@utk.edu

Amyloid-like fibrils are studied because of their significance in understanding pathogenesis and creating functional materials. Amyloid-like fibrils have been studied by heating globular proteins at acidic conditions. In the present study, intrinsically disordered α-, β-, and κ-caseins were studied to form amyloid-like fibrils at pH 2.0 and 90 ºC. No fibrils were observed for α-caseins, and acid hydrolysis was found to be the rate-limiting step of fibrillation of β- and κ-caseins. An increase of β-sheet structure was observed after fibrillation. Nanomechanic analysis of long amyloid-like fibrils using peak-force quantitative nanomechanical atomic force microscopy showed the lowest and highest Young's modulus for β-casein (2.35±0.29 GPa) and κ-casein (4.14±0.66 GPa), respectively. The dispersion with β-casein fibrils had a viscosity more than 10 and 5 times higher than those of κ-casein and β-lactoglobulin, respectively, at 0.1 s^{-1} at comparable concentrations. The current findings may assist not only the understanding of amyloid fibril formation but also the development of novel functional materials from disordered proteins.

Keywords: amyloid-like fibrils, intrinsically disordered protein, casein, nanomechanical properties, viscosity

Introduction

Amyloid fibrils formed in human tissues such as brain are significant to the understanding of pathogenesis of diseases related to neurodegenerative disorders and amyloidosis like Alzheimer's and Parkinson's diseases.[1] The formation mechanism of amyloid fibrils has been investigated extensively *in vivo* and *in vitro* with the hope to find a preventive therapy or revert fibril structures. Although it has not been identified conclusively, there are also some amyloid-like fibrils found in the mammary tissue of animals such as bovine, which cause the reduction of milk secretion. [2] It is generally believed that the formation of amyloid or amyloid-like fibrils involves the nucleation of partially unfolded proteins or peptides, followed by extension reactions to form beta-sheets through anti-parallel stacking of beta-strands by inter-strand hydrogen bonds.[3, 4]

Besides proteins related to pathogenesis, several globular proteins with a significant portion of β-sheet structures have been observed to form amyloid-like fibrils *in vitro*, such as β-lactoglobulin, yeast prions, α-lactalbumin, ovalbumin, and lysozyme.[5-11] Instead of applying physiological conditions, heating these globular proteins at acidic conditions is commonly used to form amyloid-like fibrils that can be used to unveil the fibrillation process. Studies have shown that the *in vitro* fibrillation involves steps of acid hydrolysis, nucleation and growth of acid-hydrolyzed peptides by β-sheet alignment.[6, 12] β-lactoglobulin is among the most extensively studied globular proteins and can form amyloid-like fibrils at a wide pH range below its isoelectric point (pI) of around pH 5.3 by heating.[13] A recent analysis using atomic force microscopy (AFM) demonstrated a comparable amyloidosis process between heat-denatured β-lactoglobulin and amyloidal fibrils.[14] Several parameters affect the rate and type of fibril formation. Longer fibrils are formed at a higher rate when heated at a lower ionic strength, a higher temperature, and without co-solutes such

as polysaccharides and polyols.[12, 15-18] These amyloid-like fibrils also have potential for use as functional materials to provide unique rheology, encapsulate compounds, and serve as scaffolds in tissue engineering. [9, 19, 20]

In vitro fibril formation from amorphous proteins is relatively scarce.[1] Caseins abundant in mammalian milk lack of defined three-dimensional structures and are classified as intrinsically disordered proteins. [21] Several studies have characterized the properties of bovine caseins in forming fibrils. In bovine milk, caseins consist of about 80% of proteins [22] and four types of caseins (α_{s1}, α_{s2}, β, and κ) assemble as mostly spherical colloidal particles with a diameter of 50-250 nm. [23] Caseins have less secondary or tertiary structures than globular proteins under physiological conditions and can function as molecular chaperones to stabilize proteins through electrostatic and hydrophobic interactions. [24, 25] Caseins also have numerous applications based on their balanced hydrophilicity/hydrophobicity and self-assembling properties. [26-29] κ-casein can form amyloid-like fibrils under physiological conditions with or without a reducing agent.[30] The fibrillation involves the formation of multimers from individual κ-casein molecules and conformational rearrangement to form more organized species, which subsequently undergo micellar assembling and further growing to form amyloid-like fibrils.[30, 31] The fibrillation of κ-casein can be inhibited by α_s- and β-caseins, which results in the absence of amyloid-like fibrils when different types of caseins are present under physiological conditions.[30] The fibrillation of α_{s2}-casein at physiological conditions was also observed but was inhibited by β- or α_{s1}-casein. [30, 32] These findings collectively suggest the prevention of amyloidosis accumulation in mammary tissues and the development of corpora amylacea. [30, 32] It was also observed that α_{s1}-casein inhibits fibrillogenesis of Aβ1-40, a peptide involved in Alzheimer's disease, by increasing the nucleation lag-time and slowing down the overall fibrilliation. [33] Currently, formation of amyloid-like fibrils by heating caseins at acidic conditions has not been studied.

In the present study, the objective was to study amyloid-like fibrils produced from bovine caseins by heating at 90 °C and pH 2.0, and compare their physicochemical and nanomechanical properties with fibrils formed from β-lactoglobulin. The fibrillation kinetics was monitored using Thioflavin T (Th-T) fluorescence spectroscopy for up to 48 h. The morphology of fibrils was characterized using transmission electron microscopy (TEM) and AFM). The hydrolysis kinetics was quantified using sodium dodecyl sulfate-polyacrylamide gel electrophoresis (SDS-PAGE), and changes of secondary structures were studied using Fourier transform infrared (FTIR) spectroscopy and circular dichroism (CD) spectroscopy. Finally, rheological properties of fibril dispersions formed from different proteins were characterized.

Results and discussions

Amyloid-like fibril formation kinetics

Amyloid-like fibrils are formed by sequentially stacking of beta-strands to beta-sheets perpendicularly to the main axil of the fibril. [3, 4] Because the selective binding between ThT and fibrils strengthens the emitted fluorescence intensity, the quantified fluorescence intensity can be used to monitor the growth of amyloid-like fibrils.[34, 35] Figure 1 shows the normalized ThT fluorescence intensity of samples after heating α-, β-, and κ-caseins and β-lactoglobulin for different durations. Heating α-casein at 90 °C and pH 2.0 did not change ThT fluorescence, indicating the absence of fibrils. The α-casein in the current study is a mixture of α_{s1}- and α_{s2}-caseins. The mixed α-casein does not form fibrils at physiological conditions, but the purified α_{s2}-casein does, which indicates the suppression of fibril formation from α_{s2}-casein by α_{s1}-casein.[30, 32] Unfortunately, we were not able to find purified α_{s1}- and α_{s2}-caseins to verify similar inhibition occurred during heating at pH 2.0.

κ-Casein and β-lactoglobulin showed similar and typical sigmoidal increase in ThT fluorescence intensity at extended heating durations (Figure 1). The kinetic parameters after fitting data to Eqs. 2-4 are summarized in Table 1. Both proteins reached a plateau after heating at 90 °C for 12 h, which is similar to previous studies.[10, 36] Different from κ-casein and β-lactoglobulin, β-casein showed a delayed increase in ThT fluorescence in the first 12 h and did not reach an equilibrium after 24 h. Therefore, each casein showed distinctly different properties in forming amyloid-like fibrils during heating at pH 2.0.

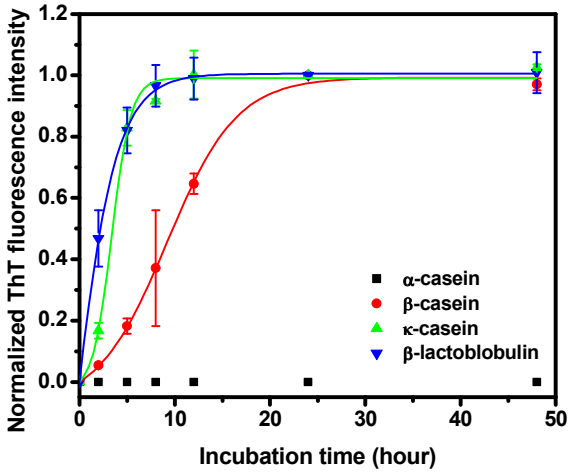

Figure 1. Normalized ThT fluorescence of α-casein, β-casein, κ-casein, and β-lactoglobulin solutions after heating at 90 °C and pH 2.0 for 0-48 h at a protein concentration of 10 mg/mL. Error bars are standard deviations from triplicates. Solid lines indicate the fitting of data to Eq. 2.

Table 1. Fibrillation parameters estimated from ThT fluorescence based on Eqs. 2-4.

Protein	t_{lag} (h)	$t_{1/2max}$ (h)	Adjusted r^2
β-casein	2.96	9.74	0.9983
κ-casein	1.51	3.45	0.9924

β-lactoglobulin	0.05	2.21	0.9994

Acid hydrolysis kinetics of proteins

The fibril formation kinetics can be affected by several parameters such as pH and temperature that determine the kinetics of acid hydrolysis, as well as nucleation and growth which are a function of both hydrolysate structures and environment conditions. [15, 37] To understand the rate-determining step during fibril formation, SDS-PAGE was used to monitor acid hydrolysis during heating (Figure 2). Hydrolysis of proteins to peptides smaller than 10 kDa mostly completed in the first 12 h, with β-casein being the slowest. The hydrolysis kinetics quantified from SDS-PAGE after fitting the model in Eq. 5 is shown in Figure 3, and the estimated rate constants are presented in Table 2. α-Casein was hydrolyzed the fastest, with a k_h of 0.332 ± 0.008 h^{-1}. κ-Casein and β-lactoglobulin showed similar hydrolysis kinetics with k_h of 0.301 ± 0.022 h^{-1} and 0.310 ± 0.015 h^{-1}, respectively. The k_h of β-casein hydrolysis (0.228 ± 0.018 h^{-1}) was significantly smaller than the other three proteins. The calculated hydrophobicity of proteins follows the decreasing order of β-casein > κ-casein = β-lactoglobulin > α_{s1}-casein > α_{s2}-casein.[38] Therefore, a more hydrophobic protein is hydrolyzed more slowly during heating at acidic conditions. This is expected because a more hydrophobic protein reduces the exposure of amide bonds for acid hydrolysis, which also is in agreement with the ThT fluorescence intensity changes (Figure 1). With the exception of α-casein (no fibril formation), acid hydrolysis is thus the rate-limiting step in fibrillation of these proteins during heating at acidic conditions.

Table 2. Protein hydrolysis rate constant (k_h) estimated from SDS-PAGE (Figure 2).

Protein	k_h (h^{-1})*	Adjusted r^2
α-Casein	0.332 ± 0.008	0.9970
β-casein	0.228 ± 0.018	0.9683
κ-Casein	0.301 ± 0.022	0.9748
β-lactoglobulin	0.310 ± 0.015	0.9889

*Data are mean ± standard error from fitting.

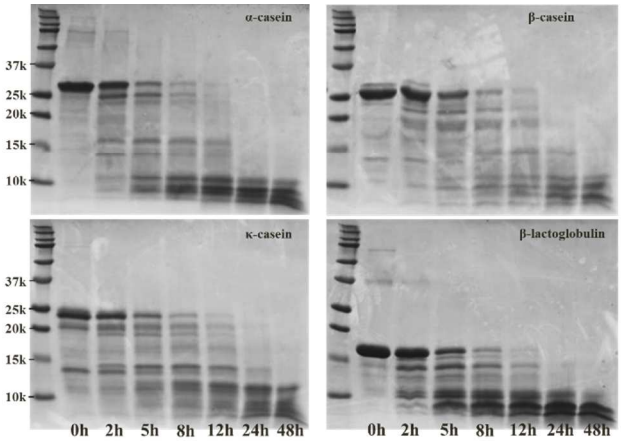

Figure 2. SDS-PAGE analysis of α-casein, β-casein, κ-casein, and β-lactoglobulin after heating at 90 °C and pH 2.0 for 0-48 h.

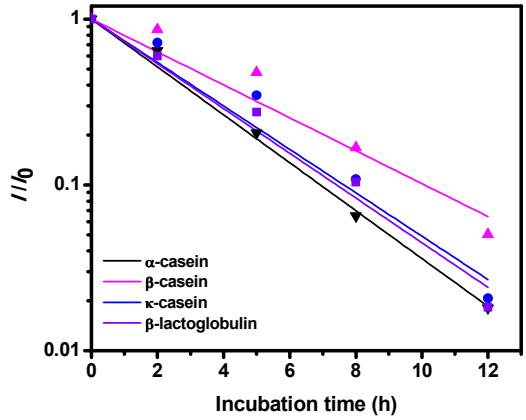

Figure 3. Normalized SDS-PAGE band intensity showing hydrolysis kinetics of α-casein, β-casein, κ-casein, and β-lactoglobulin after heating at 90 °C and pH 2.0 for up to 12 h.

Morphology and nano-mechanical properties of fibrils

The morphology of proteins after heating at 90 °C and pH 2.0 for 24 h was studied using TEM, shown in Figure 4. As indicated for absence of fibrils based on ThT fluorescence (Figure 1), individual particles and aggregates without amyloid-like fibrils were observed for α-casein (Figure 4). In contrast, amyloid-like fibrils were evident for β-casein, κ-casein, and β-lactglobulin treatments.

AFM is also commonly used to characterize the structure of amyloid-like fibrils, and the nanoscale structures facilitate the understanding of fibrillation mechanism. [13, 39] Characterization of nanoscale mechanical properties of materials is a unique feature of AFM, and the peak force value in the force-distance curves can be used to calculate Young's modulus in real time by fitting data in the Derjaguin–Mueller–Toporov model.[39, 40] Figures 5-7 show morphological and mechanical properties of β-casein, κ-casein, and β-lactoglobulin before and after incubation at pH 2.0 and 90 ºC for 24 h. All three proteins showed spherical structures before heating. After heating, amyloid-like fibrils with a length greater than 1 μm were observed. General observations showed that fibrils of β-lactoglobulin were overall longer than those of β-casein and κ-casein.

The average Young's moduli measured from different fibrils are summarized in Table 3. The Young's modulus of β-lactoglobulin fibrils (3.45 GPa) was close to the previously reported value of 3.7 GPa. [41] The Young's modulus of β-casein fibrils (2.35 GPa) was lower than that of β-lactoglobulin but was close to that of α-synulein and end-capped heptapeptide CH_3CONH-βAβAKLVFF-$CONH_2$ fibrils.[41, 42] κ-Casein fibrils had the highest modulus (4.14 GPa) among the three protein fibrils. The difference in fibril modulus can be caused by the strength of intermolecular forces and can be correlated to material stiffness. [43] These fibrils may be used to design functional materials with different mechanical properties.

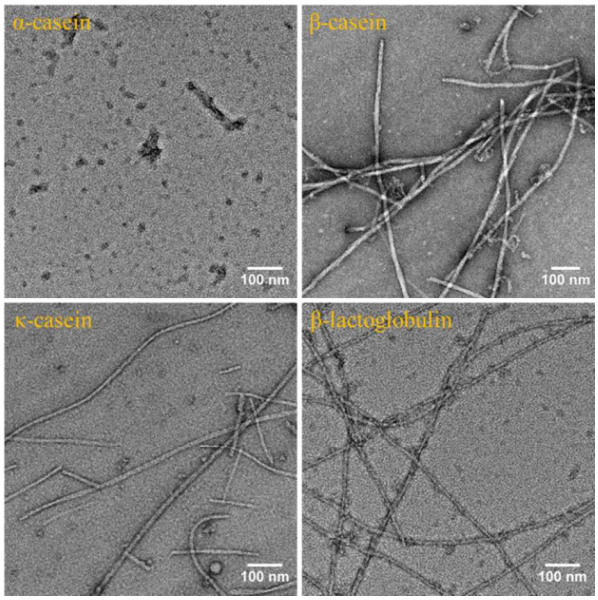

Figure 4. TEM images showing structures of α-casein, β-casein, κ-casein, and β-lactoglobulin after heating at pH 2.0 and 90 °C for 24 h.

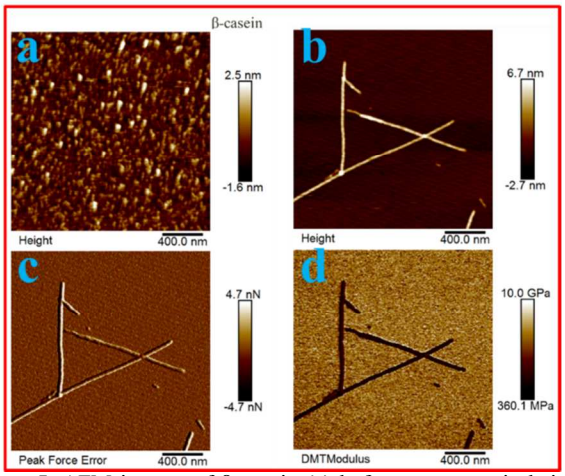

Figure 5. AFM images of β-casein (a) before treatment in height channel and after treatment in (b) height, (c) peak force error, and (d) Derjaguin-Muller-Toporov (DMT) modulus channels.

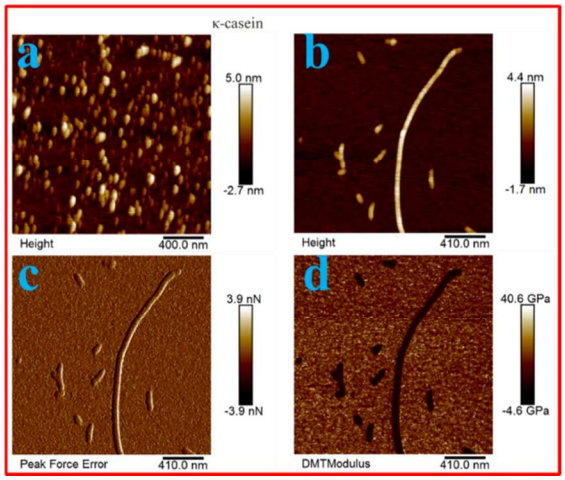

Figure 6. AFM images of κ-casein (a) before treatment in height channel and after treatment in (b) height, (c) peak force error, and (d) Derjaguin-Muller-Toporov (DMT) modulus channels.

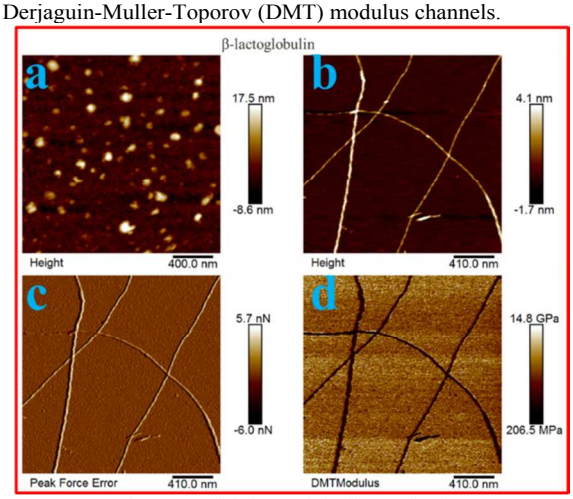

Figure 7. AFM images of β-lactoglobulin (a) before treatment in height channel and after treatment in (b) height, (c) peak force error, and (d) Derjaguin-Muller-Toporov (DMT) modulus channels.

Structural changes of proteins analyzed using FTIR and CD spectroscopy

The secondary structural changes of caseins before and after heating for 24 h were analyzed using ATR-FTIR, with the spectra presented in supplementary Figure S1. Contrasting with no changes of α-casein, IR peaks of β- and κ-caseins shifted to a lower wavenumber after heating (supplementary Figure S1), indicating the increased contents of ordered structures.[31, 44]

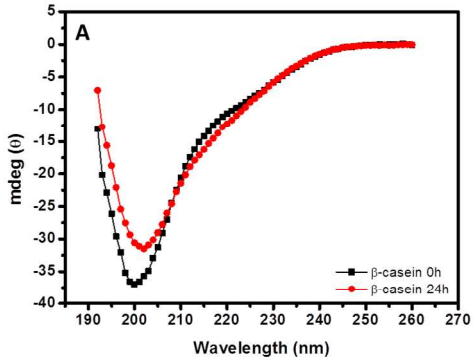

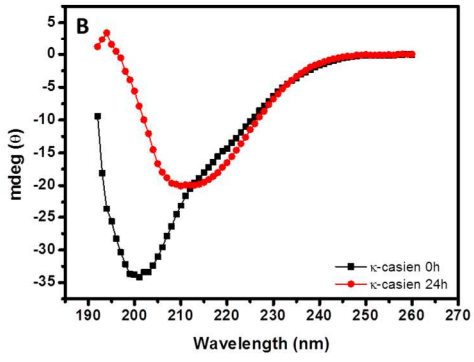

Figure 8. CD spectra of (A) β-casein and (B) κ-casein before and after heating at 90 °C and pH 2.0 for 24 h.

To confirm with ATR-FTIR results, Far-UV CD spectra of β-casein and κ-casein were measured before and after heating for 24 h (Figure 8). The large negative ellipticity centered on 200 nm and 201 nm for β-casein and κ-casein, respectively, before heating and the low ellipticity at 220 nm are characteristics of disordered structures.[24] After heating, there were redshifts of the minimum in ellipticity for β-casein and κ-casein to 202 nm and 210 nm, respectively. Coupled by the increase of ellipticity at 192-200 nm region and decrease at 210-200 nm region, the spectra indicated an increase in β-sheet and a reduced content of irregular structure after heating.[32] The greater extent of redshift observed for the CD spectrum of κ-casein after heating indicates the greater increase of contents of regular structures than β-casein.

Table 3. Average Young's modulus of β-casein, κ-casein, and β-lactoglobulin fibrils produced by heating at 90 °C and pH 2.0 for 24 h measured using atomic force microscopy operated in quantitative nanomechanics mode.

Protein	Young's Modulus (GPa)*
β-casein	2.35 ± 0.29^{c}
κ-casein	4.14 ± 0.66^{a}
β-lactoglobulin	3.45 ± 0.67^{b}

*Data are mean ± standard deviation from 100 fibrils.

Rheological property of fibril dispersions

Viscosity is an important property to assess the potential of materials in applications such as texture modifiers or adhesives.[45] The viscosity of all protein samples increased after heating for 24 h, which has also been observed in other fibril systems.[10, 18] The increased viscosity can be explained by the increased mass and hydrodynamic diameter of amyloid-like fibrils after acid hydrolysis and structure assembly.[10, 46, 47] The apparent viscosity of κ-casein fibril dispersion at 0.1 s^{-1} (~0.1 Pa-s) was about one-half of the β-lactoglobulin fibril sample. The β-casein fibril dispersion showed the highest viscosity and was more than one decade higher than the viscosity of κ-casein fibril dispersion at 0.1 s^{-1}. There was a negative correlation between Young's modulus and viscosity among β-casein, κ-casein, and β-lactoglobulin ($p < 0.05$). For a model system studied with actin, the maximum shear strain that a network can withstand was found to decrease with the increase of modulus or chain stiffness, and vice versa. [48] Therefore, this correlation may be interpreted by the flexibility of fibrils that is negatively correlated to Young's modulus (Table 1).

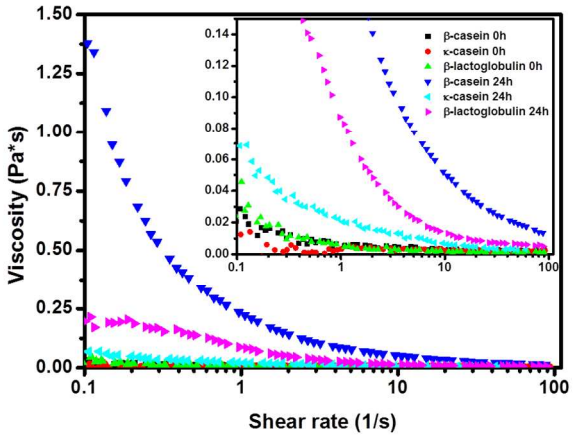

Figure 9. Viscosity of dispersions with 10 mg/mL β-casein, κ-casein, and β-lactoglobulin before and after heating at 90 °C and pH 2.0 for 24 h. The inset shows the partial data up to 0.15 Pa-s.

Conclusions

In conclusion, the present study suggests for the first time that amyloid-like fibrils can be formed from β- and κ-caseins in a controlled manner during heating at acidic pH, especially β-casein that has long been used as a molecular chaperone to inhibit the formation of amyloid-like fibrils *in vitro*. The fibrillation of caseins was limited by the acid hydrolysis rate and resulted in more organized structures with increased contents of β-sheet. Fibrils of β- and κ-caseins differed in nanomechanical properties and bulk viscosity, suggesting the potential of κ-casein fibrils as novel biomaterials to provide mechanical strength and β-casein fibrils as an effective texture modifier or adhesive. The current findings may be important to not only the enhanced understanding of amyloid formation but also the exploration of novel biomaterials.

Experimental methods

Chemicals

α-, β-, and κ-caseins and β-lactglobulin were purchased from Sigma Aldrich Corp. (St. Louis, MO) and were used without further purification. Polyacrylamide gels and protein markers were purchased from Bio-Rad Laboratories Inc. (Hercules, CA). Dialysis tubing with a nominal molecular weight cutoff (MWCO) of 6000-8000 Da and β-mercaptoethanol were purchased from Sigma-Aldrich Corp. (St. Louis, MO). Other chemicals were of analytical grade and were purchased from Fisher Scientific, Inc. (Pittsburgh, PA).

Preparation of fibrils

Each protein was dissolved at 10 mg/mL in deionized water, and the pH was adjusted to 2.0 using 1.0 M HCl. Samples were heated at 90 °C for up to 48 h by incubating in the glycerol bath heated on a hot magnetic stir pate

operating at 300 rpm. Samples were transferred and quenched in an ice bath at pre-determined time intervals.

Thioflavin T (ThT) fluorescence spectroscopy

The ThT fluorescent properties of samples were characterized using spectrofluorometry (model RF-1501, Shimadzu Corp., Tokyo, Japan) as an indicator of fibril formation.[34, 35] 50 μL of a protein sample was mixed with 5 mL of the ThT working solution (0.8 mg/mL). The emission spectra at a range of 460−700 nm were acquired using an excitation wavelength of 440 nm. The fluorescence of protein samples was calibrated by subtracting the background of the ThT working solution without protein. The maximum fluorescence intensity of a sample (F_m) was used to calculate the normalized intensity by that of the same protein sample produced after 24-h heating (F_{24}) that showed the highest intensity among the time points:

$$\text{Normalized intensity} = \frac{F_m - F_0}{F_{24} - F_0} \quad (1)$$

where F_o is the maximum fluorescence intensity of a sample before heating.

The ThT fluorescence data were fitted with the following model: [12, 49]

$$f_t = \alpha - \frac{\frac{\beta}{\gamma}+\alpha}{1+\frac{\beta}{\alpha\gamma}\exp[t(\beta+\alpha\gamma)]} \quad (2)$$

where f_t is the normalized fluorescence intensity at time t, and α, β, and γ are arbitrary constants. The lag phase length (t_{lag}) and the time required to reach one-half of the maximum fluorescence ($t_{1/2max}$) were calculated using Eq. (3) and (4), respectively.

$$t_{lag} = \frac{1}{\beta+\alpha\gamma}\left(\ln\left(\frac{\alpha\gamma}{\beta}\right) - 4\frac{\alpha\gamma}{\beta+\alpha\gamma} + 2\right) \quad (3)$$

$$t_{1/2max} = \frac{\ln\left(2+\frac{\alpha\gamma}{\beta}\right)}{\beta+\alpha\gamma} \quad (4)$$

Transmission electron microscopy (TEM)

The morphology of fibrils produced after 24-h heating was studied using TEM. The freshly prepared sample was diluted 100 times with deionized water. One drop of a diluted sample was placed on a freshly glow-discharged carbon film on a 400-mesh copper grid and then stained with 1% uranyl acetate. Samples were imaged with a Zeiss Libra TEM operating at 200 kV (Carl Zeiss Microscopy, Oberkochen, Germany).

Atomic force microscopy (AFM)

The topography and nano-mechanical properties of fibrils were characterized using AFM. 10 μL of a 200-fold diluted sample was spread evenly onto a freshly cleaved mica sheet mounted on a sample disk (Bruker Corp., Santa Barbara, CA), and was rinsed with 1 mL deionized water previously adjusted to pH 2.0 after incubation at room temperature for 1 minute. A rectangular cantilever having an aluminum reflective coating on the backside and a quoted force constant of 40 N/m (RTESPA, Bruker Corp.) was used on a Multimode VIII microscope (Bruker AXS, Billerica, MA). The peak-force quantitative nanomechanical mode was used to scan the sample, [41, 50] and topography images were generated with a preset scan area of 2.0×2.0 μm at a scanning speed of 1 Hz. A relative method was used to calibrate the cantilever on the polystyrene film with a 2.7 GPa nominal modulus.

Sodium dodecyl sulfate-polyacrylamide gel electrophoresis (SDS-PAGE)

A precast 15% gradient polyacrylamide gel from Bio-Rad Laboratories, Inc. (Hercules, CA) was used in SDS-PAGE. 40 μL of a protein sample was mixed with 200 μL of a SDS-PAGE sample buffer (catalog number MB01015, GenScript Corp., Piscataway, NJ). After heating at 95 °C for 5 min, 10 μL of each sample was loaded to the gel well for electrophoresis at 200 V till the indicator dye reached the gel bottom. The intensity of the band corresponding to each protein after heating (I) for a duration of t was quantified using ImageJ software (NIH, Bethesda, MD) and was normalized by the intensity of unheated protein (I_o) run on the same gel. The data were analyzed using the first-order kinetics: [12]

$$I = I_o * e^{-k_h * t} \quad (5)$$

where k_h is the hydrolysis rate constant.

Circular dichroism (CD) spectroscopy.

The instrument used in the far-UV CD spectroscopy was a Jasco model J-815 CD spectrometer (Jasco, Inc., Easton, MD). Fibrils were dialyzed using a membrane with a MWCO of 6000-8000 Da at 4 °C for 4 days with mild stirring against water acidified to pH 2.0. The concentrations of proteins and fibrils were measured using the bichinconinic acid assay method after 10-fold dilution in deionized water previously adjusted to pH 2. The diluted sample was scanned 10 times at a rate of 50 nm/min from 192 to 260 nm with a bandwidth of 1 nm.

Fourier-transform infrared spectroscopy (FTIR)

The structural changes of caseins before and after heating at 90 °C for 24 h were studied for FTIR following previously reported methods with modifications. [44, 51] Briefly, the liquid samples after dialysis as above were dried on a mica surface and the spectra were acquired using an ATR-FTIR Nicolet Nexus 670 IR spectrometer (Thermo Nicolet Corp., Madison, MI) which was equipped with a Germanium attenuated total reflection (ATR) accessory. The IR transmittance was acquired from 1600 to 1700 cm^{-1} with a resolution of 2 cm^{-1}. 100 repeated scans were undertaken for each sample. All signals were collected against a background spectrum recorded from the mica substrate only.

Rheology

The viscosity of samples before and after heating was measured using a stress-controlled rheometer (model AR2000, TA Instruments Inc., New Castle, DE). The cone-plate geometry with a cone angle of 1° and a cone diameter of 40 mm was used in shear rate ramps from 0.1 to 100 s^{-1} at 25 °C.

Statistical analysis

Statistical analyses were performed using the SAS program (version 9.3, SAS Institute, Cary, NC). One-way analysis of variance (ANOVA) was carried out. Differences between pairs of means were compared using a Tukey's test. The significance level was set at 0.05.

Acknowledgement

This work was supported by the University of Tennessee and the USDA National Institute of Food and Agriculture Hatch Project 223984.

Notes and references

1 V. N. Uversky, *Curr. Alzheimer Res.*, 2008, **5**, 260.
2 S. C. Nickerson, L. M. Sordillo, N. T. Boddie and A. M. Saxton, *J. Dairy Sci.*, 1985, **68**, 709.
3 R. S. Harrison, P. C. Sharpe, Y. Singh and D. P. Fairlie, in *Reviews of Physiology, Biochemistry and Pharmacology*, eds. S. G. Amara, E. Bamberg, B. Fleischmann, T. Gudermann, S. C. Hebert, R. Jahn, W. J. Lederer, R. Lill, A. Miyajima, S. Offermanns and R. Zechner, Springer-Verlag Berlin, Berlin, 2007, vol. 159, pp. 1-77.
4 M. Stefani, *Biochim. Biophys. Acta-Mol. Basis Dis.*, 2004, **1739**, 5.
5 C. Lara, S. Handschin and R. Mezzenga, *Nanoscale*, 2013, **5**, 7197.
6 C. Lara, J. Adamcik, S. Jordens and R. Mezzenga, *Biomacromolecules*, 2011, **12**, 1868.
7 T. R. Serio, A. G. Cashikar, A. S. Kowal, G. J. Sawicki, J. J. Moslehi, L. Serpell, M. F. Arnsdorf and S. L. Lindquist, *Science*, 2000, **289**, 1317.
8 J. Goers, S. E. Permyakov, E. A. Permyakov, V. N. Uversky and A. L. Fink, *Biochemistry*, 2002, **41**, 12546.
9 N. P. Reynolds, M. Charnley, R. Mezzenga and P. G. Hartley, *Biomacromolecules*, 2014, **15**, 599.
10 G. Liu and Q. X. Zhong, *Biomacromolecules*, 2013, **14**, 2146.
11 O. G. Jones and R. Mezzenga, *Soft Matter*, 2012, **8**, 876.
12 A. C. Dave, S. M. Loveday, S. G. Anema, G. B. Jameson and H. Singh, *Biomacromolecules*, 2014, **15**, 95.
13 W. S. Gosal, A. H. Clark, P. D. A. Pudney and S. B. Ross-Murphy, *Langmuir*, 2002, **18**, 7174.
14 J. Adamcik, J. M. Jung, J. Flakowski, P. De Los Rios, G. Dietler and R. Mezzenga, *Nat. Nanotechnol.*, 2010, **5**, 423.
15 O. G. Jones, J. Adamcik, S. Handschin, S. Bolisetty and R. Mezzenga, *Langmuir*, 2010, **26**, 17449.
16 C. Lara, S. Gourdin-Bertin, J. Adamcik, S. Bolisetty and R. Mezzenga, *Biomacromolecules*, 2012, **13**, 4213.
17 S. Bolisetty, L. Harnau, J. M. Jung and R. Mezzenga, *Biomacromolecules*, 2012, **13**, 3241.
18 S. M. Loveday, J. H. Su, M. A. Rao, S. G. Anema and H. Singh, *Biomacromolecules*, 2011, **12**, 3780.
19 K. N. P. Humblet-Hua, G. Scheltens, E. van der Linden and L. M. C. Sagis, *Food Hydrocolloids*, 2011, **25**, 307.
20 J. F. Graveland-Bikker and C. G. de Kruif, *Trends Food Sci. Technol.*, 2006, **17**, 196.
21 R. van der Lee, M. Buljan, B. Lang, R. J. Weatheritt, G. W. Daughdrill, A. K. Dunker, M. Fuxreiter, J. Gough, J. Gsponer, D. T. Jones, P. M. Kim, R. W. Kriwacki, C. J. Oldfield, R. V. Pappu, P. Tompa, V. N. Uversky, P. E. Wright and M. M. Babu, *Chem. Rev.*, 2014, **114**, 6589.
22 P. F. Fox, in *Advanced Dairy Chemistry: Proteins*, ed. P. F. Fox, Elsevier, New York, NY, 3rd edn., 2003, vol. 1, pp. 1-41.
23 P. Udabage, I. R. McKinnon and M. A. Augustin, *J. Dairy Res.*, 2003, **70**, 453.
24 V. N. Uversky, *Eur. J. Biochem.*, 2002, **269**, 2.
25 J. A. Carver, A. Rekas, D. C. Thorn and M. R. Wilson, *IUBMB Life*, 2003, **55**, 661.
26 M. Esmaili and S. M. Ghaffari, *LWT-Food Sci. Technol.*, 2011, **44**, 2166.
27 K. Pan, H. Chen, P. M. Davidson and Q. Zhong, *J. Agric. Food Chem.*, 2014, **62**, 1649.
28 K. Pan, Y. Luo, Y. Gan, S. J. Baek and Q. Zhong, *Soft Matter*, 2014, **10**, 6820.
29 K. Pan, Q. Zhong and S. J. Baek, *J. Agric. Food Chem.*, 2013, **61**, 6036.
30 D. C. Thorn, S. Meehan, M. Sunde, A. Rekas, S. L. Gras, C. E. MacPhee, C. M. Dobson, M. R. Wilson and J. A. Carver, *Biochemistry*, 2005, **44**, 17027.
31 J. Leonil, G. Henry, D. Jouanneau, M. M. Delage, V. Forge and J. L. Putaux, *J. Mol. Biol.*, 2008, **381**, 1267.
32 D. C. Thorn, H. Ecroyd, M. Sunde, S. Poon and J. A. Carver, *Biochemistry*, 2008, **47**, 3926.
33 R. Carrotta, C. Canale, A. Diaspro, A. Trapani, P. L. San Biagio and D. Bulone, *Biochim. Biophys. Acta-Gen. Subj.*, 2012, **1820**, 124.
34 M. Torok, S. Milton, R. Kayed, P. Wu, T. McIntire, C. G. Glabe and R. Langen, *J. Biol. Chem.*, 2002, **277**, 40810.
35 T. Ban, D. Hamada, K. Hasegawa, H. Naiki and Y. Goto, *J. Biol. Chem.*, 2003, **278**, 16462.
36 S. M. Loveday, X. L. Wang, M. A. Rao, S. G. Anema, L. K. Creamer and H. Singh, *Int. Dairy J.*, 2010, **20**, 571.
37 M. R. H. Krebs, G. L. Devlin and A. M. Donald, *Biophys. J.*, 2009, **96**, 5013.
38 L. C. Chaplin, *J. Chromatogr.*, 1986, **363**, 329.
39 J. Adamcik and R. Mezzenga, *Curr. Opin. Colloid Interface Sci.*, 2012, **17**, 369.
40 F. J. G. de Abajo and J. Aizpurua, *Phys. Rev. B*, 1997, **56**, 15873.
41 J. Adamcik, C. Lara, I. Usov, J. S. Jeong, F. S. Ruggeri, G. Dietler, H. A. Lashuel, I. W. Hamley and R. Mezzenga, *Nanoscale*, 2012, **4**, 4426.

42 K. Sweers, K. van der Werf, M. Bennink and V. Subramaniam, *Nanoscale Res. Lett.*, 2011, **6**, 1.
43 T. P. J. Knowles and M. J. Buehler, *Nat. Nanotechnol.*, 2011, **6**, 469.
44 H. Hiramatsu and T. Kitagawa, *BBA-Proteins Proteomics*, 2005, **1753**, 100.
45 L. M. Sun, S. J. Yi, Y. Z. Wang, K. Pan, Q. X. Zhong and M. J. Zhang, *Bioinspir. Biomim.*, 2014, **9**, 1.
46 G. Robinson, S. B. Rossmurphy and E. R. Morris, *Carbohydr. Res.*, 1982, **107**, 17.
47 O. Smidsrød and A. Haug, *Biopolymers*, 1971, **10**, 1213.
48 F. C. Mackintosh, J. Kas and P. A. Janmey, *Phys. Rev. Lett.*, 1995, **75**, 4425.
49 A. M. Morris, M. A. Watzky, J. N. Agar and R. G. Finke, *Biochemistry*, 2008, **47**, 2413.
50 J. Adamcik, A. Berquand and R. Mezzenga, *Appl. Phys. Lett.*, 2011, **98**, 193701-1.
51 H. M. Farrell, E. D. Wickham, J. J. Unruh, P. X. Qi and P. D. Hoagland, *Food Hydrocolloids*, 2001, **15**, 341.